Research Article

Fazal Suhrab Gul, Muhammad Azeem, Mohsan Nawaz, Zia Ur Rehman*, Sara A. Alqarni, Attiq Ur Rehman, Antonio Miotello, Akhtar Munir, Khalid Ali Khan and Magdi E.A. Zaki*

Low molar mass ionic liquid's modified carbon nanotubes and its role in PVDF crystalline stress generation

https://doi.org/10.1515/ntrev-2025-0226
Received November 9, 2024; accepted September 22, 2025; published online December 8, 2025

Abstract: In this work, the question is whether the positive charge or the confirmation of side chain of an ionic liquid l-methylimidazolium bromide or the modified solid support multi-walled carbon nanotubes affects the heterogeneous crystallization of melt-crystallized polyvinylidene fluoride. The percentage (%) weight of polyvinylidene fluoride, ionic liquid and multi-walled carbon nanotubes were sequentially dissolved into DMF and stirred for 2 h at 40 °C. The homogeneous solutions were poured into petri-dishes to solidify. The samples P0, P1, P2, P3, P4, P5 were characterized via FTIR, SEM, DSC and XRD. The data obtained solidly supported the investigation. The concentration of ionic liquid was optimized according to the system employed. It was confirmed that multi-walled carbon nanotubes accelerate heterogeneous nucleation of polyvinylidene fluoride as usual, but the formed crystals are dominantly nonpolar α form. Incorporation of only ionic liquid results in depression of the polyvinylidene fluoride melting crystallization rate due to the inherent plasticity of ionic liquid but generates higher content of polar β and γ crystals. The structural spherulites were deformed in case of ionic liquid utilization. The ionic liquid's loaded solid supports multi-walled carbon nanotubes synergistically enhancing both nucleation and polar phase formation. The immiscibility and non-compatibility of the ionic liquid generated a unique stressed structure with delayed crystallization in the form of necklace-like structure on the composite surface clearly depicted from SEM data.

Keywords: pristine multiwalled carbon nanotubes; polyvinylidene fluoride; crystallization behavior; nucleation agent; polar crystals; synergetic effects

***Corresponding authors: Zia Ur Rehman**, Department of Chemistry, Hazara University, Mansehra 21120, Khyber Pakhtunkhwa, Pakistan; and Institute of Advanced Materials, College of Material Science & Engineering, Jiangsu University, Zhenjiang, 212013, China, E-mail: ziamwt1@gmail.com; and **Magdi E.A. Zaki**, Department of Chemistry, College of Science, Imam Mohammad Ibn Saud Islamic University (IMSIU), Riyadh 11623, Saudi Arabia, E-mail: mezaki@imamu.edu.sa
Fazal Suhrab Gul, Muhammad Azeem and Mohsan Nawaz, Department of Chemistry, Hazara University, Mansehra 21120, Khyber Pakhtunkhwa, Pakistan
Sara A. Alqarni, Department of Chemistry, College of Science, University of Jeddah, Jeddah, Saudi Arabia
Attiq Ur Rehman, School of Chemistry and Chemical Engineering, Jiangsu University, Zhenjiang, 212013, China
Antonio Miotello, Department of Physics, University of Trento, Via Sommarive 14, 38123 Trento, Italy
Akhtar Munir, Department of Chemistry, Quaid-i-Azam University, Islamabad 45320, Pakistan
Khalid Ali Khan, Applied College, Center of Bee Research and its Products (CBRP), King Khalid University, P.O. Box 9004, Abha 61413, Saudi Arabia

1 Introduction

Poly (vinylidene fluoride) a fluorinated polymer, commonly abbreviated as "PVDF" is a semi-crystalline electroactive material with a low glass transition (T_g) of −35 °C [1]. During the last three decades, researchers have given much attention to PVDF due to its incomparable characteristics of chemical resistance, high piezo- and pyro-electric coefficients [2–4]. PVDF shows five crystalline phases, such as polar beta- (β), non-polar alpha- (α) and sigma- (δ), and polar gamma- (γ) phases [5] The polar and non-polar characters arise from the skeletal orientation of the H–C–F bond. Vinylidene fluoride monomer typically polymerizes into the non-polar α-phase. Therefore, the only option utilized by researchers for achieving polar phases is the modulation of processing conditions including annealing, crystallization from solution [6, 7], strong electric field [8], mechanical deformation [9] and stretching of the thin polymer film etc., [10]. Alternatively, many researchers used substrate [11] as nucleating agents, including nanoparticles [12–14], carbon nanostructures [15–18] to nucleate polar PVDF preferably in the β form, which is mechanically strong but some time

mixture of β and γ phases are generated that leads to creation of micro-stresses with ultimate loss of mechanical strength. The polar fraction formed from the in case of filler is insignificant. In most cases 5 % of the nano-filler yield about 50 % of the polar polymorph but compatibility between polymer matrix and nanofiller and along with its segregation is still a problem to solve. On the other hand, the incorporation of only polar additives like ionic liquids also yield polar PVDF, but at the expense of loss in mechanical strength [19, 20]. Therefore, to circumvent both issues simultaneously, the surface of carbon-based reinforcement was modified (covalently and non-covalently) with polar additives like ionic liquids [21–23]. It is believed that covalent attachment of polar molecules to carbon support (nanotubes or graphene) may disrupt the extended π conjugation system of these materials, which was not traced in the non-covalently functionalized support. On the contrary, it was hypothesized that non-covalent functionalization creates synergistic forces to operate [24]. Xing et al. physically modified multi-walled carbon nanotubes MWCNTs with hydrophobic ionic liquid (IL) (1-butyl-3-methylimidazolium hexafluorophosphate) [C_4mim-PF_6] for the purpose of establishing intimate contact between solid support and polymer [25–27]. The presence of [PF_6] anion makes the ionic liquid fully compatible with the polymer and MWCNTs with achievement of 100 % β phase. The literature reveals that positive charge center in the imidazolium cation is responsible for the conversion of α to β phase [28]. We believe that only positive charge is not sufficient to transform α to β while three agents include positive (+ve) charge, hydrophilicity/hydrophobicity of the charge center and the carbon chain length of imidazolium based ionic liquid. It is believed that the butyl chain and hydrophobicity both are necessary to obtain β phase otherwise mixture will be produced.

This study was designed to filter out the effects responsible for conversion of α to β. We modified the multiwalled carbon nanotubes (MWCNTs) with a hydrophilic room-temperature ionic liquid (IL), 1-methylimidazolium bromide containing imidazolium cation with small methyl branch.

2 Experimental

2.1 Materials

The PVDF pellets of 180,000 g/mol were obtained from Sigma Aldrich, Germany. The multiwalled carbon nanotubes (CNTs) were obtained from Sigma Aldrich, Germany, with diameter: 13 nm and length: 2.5–20 μm. Ionic liquid, 1-Methylamidazoleum bromide was purchased from ioLitec, Germany. DMF was purchased from Sigma Aldrich, Germany. All the chemicals were used as received.

Table 1: Compositional recipe of the nanocomposites

S. No.	Sample code	%Wt (PVDF)	%Wt (IL)	%Wt (MWLNTS)
1	P0	100	0	0
2	P1	99	0	1
3	P2	90	10	0
4	P3	89	10	1
5	P4	86	13	1
6	P5	84.8	14.2	1

2.2 Methods

Different samples were prepared via solution casting with solvent evaporation method such as: The ingredients; PVDF, IL and MWCNT were sequentially dissolved into DMF and stirred for 2 h at 40 °C. The homogeneous solutions were poured into petri-dishes to solidify. The films thus prepared were characterized through different techniques. The ratio of ingredients is given in Table 1.

2.2.1 Modification of MWCNT

To create a positive charge center on the surface of MWCNTs and establish interaction of 1-methylimidazolium cation with the π electron cloud of MWCNTs it was coated with IL. The presence of IL may perform two functions of tubes segregation and charge creation. The presence of bromide anion makes the IL hydrophilic in hydrophobic system of PVDF and MWCNTs. This difference has generated incompatibility in the system which produced perturbed structure as seen in the SEM micrographs. It is conceptually represented in Figure 2.

The imidazolium cation of IL possesses a localized positive (+ve) charge at the C_2–H position (Figure 1). This charge electrostatically interacts with the strongly electronegative(−ve) F atom in PVDF CF_2 groups. This interaction destabilized the non-polar *tran-gauche* (TGTG') conformation of the alpha-phase and favours the all-trans (TTT)

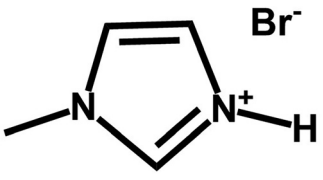

Figure 1: Structure of 1-methylimidazolium bromide.

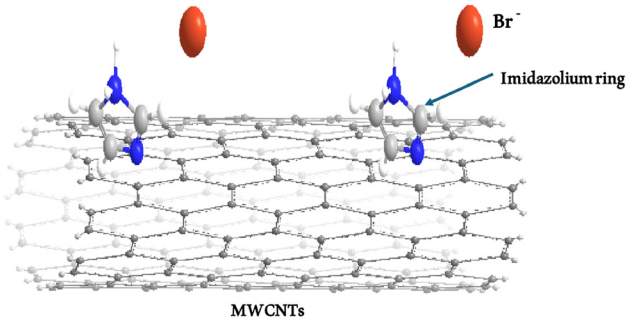

Figure 2: Graphical representation of IL modification of MWCNTs.

conformation of the beta-phase or the TTTG conformation of the gemma-phase.

3 Results and discussion

3.1 Morphological analysis

The morphological analysis was done via JEOL JSM-6490A, made in Japan. The neat PVDF films were crystalized/cooled into liquid nitrogen to avoid the generation of necking before surface morphological investigation. These films (P0, P1, P2, P3, P4 and P5) were subjected to surface analysis through electron microscopy. The micrographs were taken and depicted in Figure 3.

The micrograph shows representative morphology of the spherulites. In the case of P0 the size of spherulites is comparatively small and reflects homogeneous nucleation. This film originated from the solution of PVDF and DMF with no impurity. Thus, giving rise to the establishment of competition between the polymer chains to become stress and entangled once cooled. In case of P1, the presence of MWCNTs has taken the role of nucleating agent giving birth to bigger spherulites with inward drift in the center. This behavior indicates that as the mass of the spherulites increases, the polymer chain attached to the CNTs was attracted inward creating this trench, supporting the nucleation due to solid support with encapsulation of the CNTs with the spherulite. Such morphology can be seen in the case of accelerated crystallization or in other words heterogeneous crystallization at high temperature due to sol [29]. SEM image of PVDF/MWCNT nanocomposites reveals spherulitic structure, which is common to both α and β/γ phases [30]. The situation in the sample P2 is altogether changed, with crystal distortion and appearing in three arms fingers like structure. It means the spherulites formation was retarded, by the IL present in the melt matrix. The IL is already reported to act as plasticizer, impacting crystallization of the polymer. The increase in polarity of

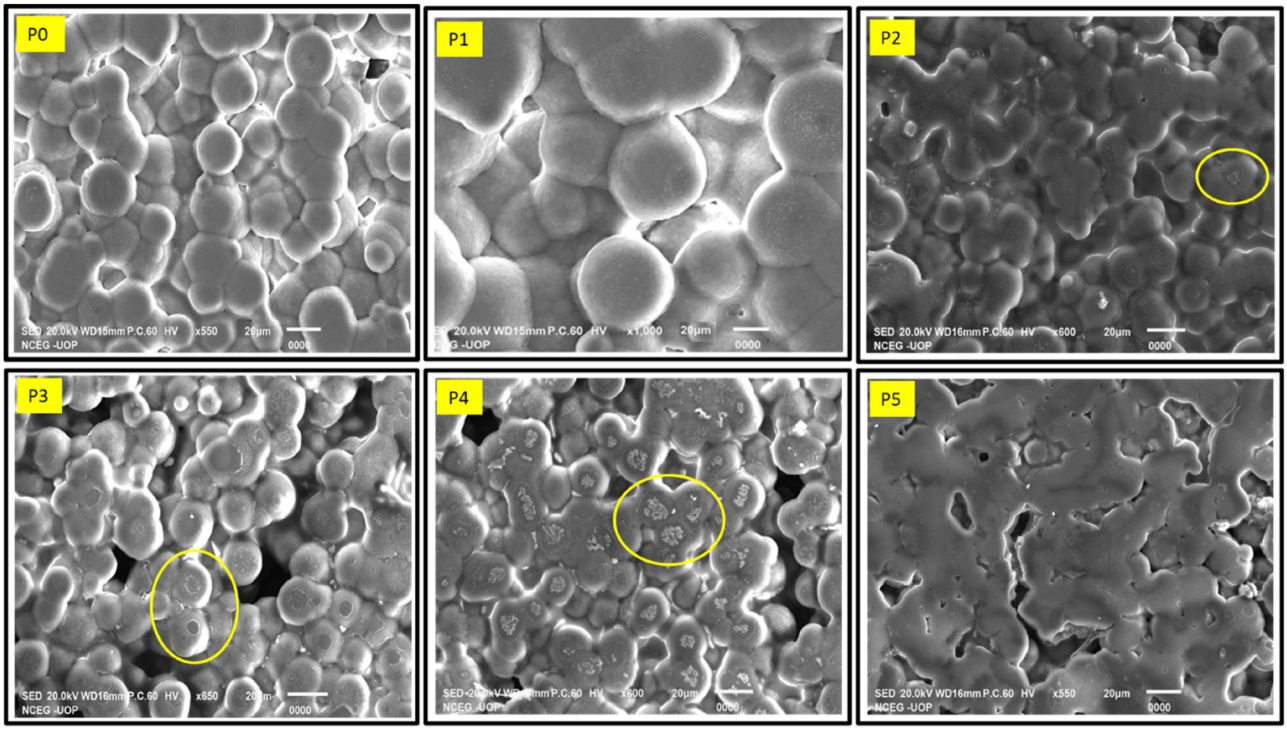

Figure 3: Morphology of, P0, P1, P2, P3, P4 and P5 at magnification of 20 μm.

the matrix due to the imidazolium cation and bromide anion create polarity gradient, thus generating β/γ phases [31–33]. The mixture of these phases is incompatible with one another and upon crystallization tends to affect one another. It is that known DMF was used in the processing step, which during crystallization de-mixed and leaves behind small pores [25, 34]. The incompatibility of IL with MWCNTs is because an integral part of IL is the hydrophilic anion [Br^{-1}] and the hydrophobic MWNCTs and PVDF push it outward of the interface when come in contact, as clearly depicted in SEM micrographs P2, P3, P4 (circle area) and appear as delayed crystal on the surface of the PVDF matrix in the form of necklace-like structure as seen in salts crystallization. In the case of P5 sample high concentration of IL, again altered the nature of the polymeric crystal with very diffused structure. The incompatible and charged nature of the IL paves way for producing stressed structures. Among other techniques FTIR and XRD were employed to clear the picture formed thus far.

3.2 FTIR analysis of polymorphism and functionality

FTIR analysis was done via Perkin Elmer FT-ATR Spectrometer. Co, USA. All samples were processed in the same way for recording of FT-IR spectra. The signals from the sample labelled as **P0** are centered at 409, 430, 479, 508, 605, 773, 830, 876, 1,071, 1,162, 1,232, 1,398, 1,405; **P1:** 410, 431, 479, 509, 609, 775, 831, 1,072, 1,165, 1,229, 1,335, 1,402; **P2:** 409, 615, 829, 1,080, 1,232, 1,335; **P3:** 425, 473, 502, 621, 829, 865, 1,066, 1,161, 1,227, 1,322, 1,399; **P4:** 408, 471, 505, 619, 658, 831, 875, 1,068, 1,161, 1,226, 1,329, 1,398, 1,546, 1,581, 1,625, 2,852, 2,972, 3,140, 3,292; **P5:** 408, 432, 474, 508, 603, 665, 755, 812, 836, 879, 1,072, 1,165, 1,232, 1,407, 1,554, 1,635, 2,854, 2,935, 3,149, 3,404 cm^{-1}. Shown in Figure 4. The α-phase of PVDF presents exclusive bands at 409, 430, 479, 508, 605, 773, 833, 876, 1,071, 1,167, 1,232, 1,398, 1,405 cm^{-1} with slight variation against the already reported data [35]. The variation may have originated from the synthetic method, which is different in each production's industry. In fact, the stable trans configuration into cis, extra amount of energy or new surface is required to stabilize the polar β phase.

At any instant when this twisting of the α-chain into β occurs, if not supported by the environment, it settled in the form of γ. In the case of P1 (410, 431, 479, 509, 609, 775, 831, 1,072, 1,165, 1,229, 1,335, 1,402), where carbon nanotubes were inserted, the signal is shifted towards higher values as seen in the data and supporting the idea that γ phase is generated while strengthening the amorphous fraction in the composites [36, 37] on the other hand, in case of P2, where the peaks born at 409, 615, 829, 1,080, 1,232, 1,335 cm^{-1} also support formation of γ phase. Here the exclusive peak due to

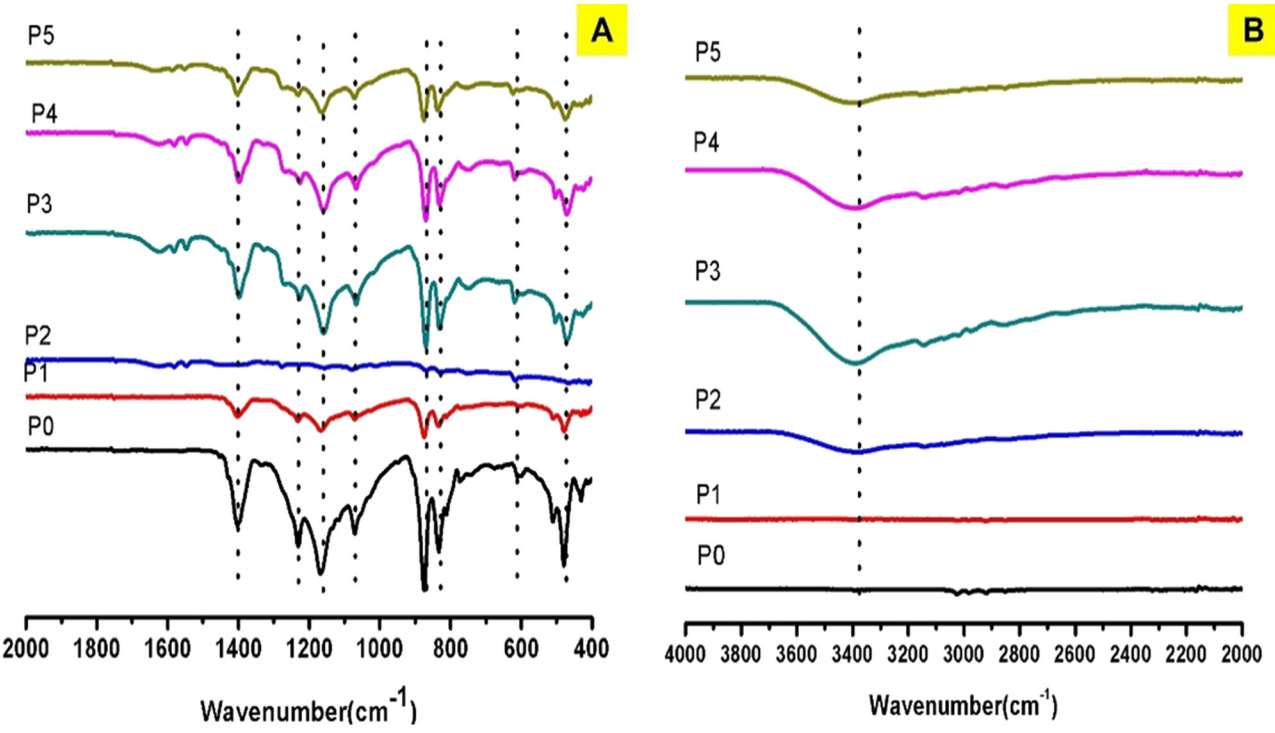

Figure 4: FTIR spectra reflecting phases of PVDF and its nanocomposites (a) 2,000–400 cm^{-1} (b) 4,000–2,000 cm^{-1}.

reported γ at 1,232 cm^{-1} as well as due to imidazolium nitrogen at 1,080 cm^{-1} can be seen. It has been experimentally observed that β phase is mechanically stiff while γ is mechanically tough. Some authors reported that peaks at or near 1,071, 1,176, and 1,402 cm^{-1} are assigned to the piezoelectric β phase, which is reflected in the case of all samples. The peak at 1,071 cm^{-1} is shifted to higher value. It can be deduced from the data presented that the insertion of the MWCNTs and ionic liquid favor the enhancement of molecular order, strengthening the intermolecular forces (converting amorphous into crystalline fraction) with high bond strength, thus pushing the IR vibration frequency to higher value as can be observed in P1–P4. Another issue is the compatibility of the ionic liquid, which can be confirmed from the data presented under the label P5. In P5, the signals at 408, 432, 474, 508, 603, 665, 755, 836, 879, 1,072, 1,165, 1,232, 1,407, 1,554, 1,635, 2,854, 2,935, 3,149, 3,404 cm^{-1} is suggestive of the fact that, although IL has played its role positive charge with no chirality or stereocenter, essential for β fraction generation. An integral part of ionic liquid is the hydrophilic anion [Br^{-1}], which makes it incompatible at the interface while the hydrophobic MWNCTs and PVDF push it outside of the interface when come in contact and, as by the in all composite samples, the C–H stretching vibrations at 2,800–3,000 cm^{-1} are seen in neat polymer as well as in composites, reflecting the development of interactive forces to develop between the ingredients. Conclusively, it can be inferred from the afore discussion that the existence of only positive charge is sufficient to create γ form but no β, because for the later to obtain conformational alignment of the substrate or entity at the interface are essential components to match. It was also reported that signals due to γ polymorph is difficult to distinguish from the α-crystal. In fact, DMF was used in the sample preparation step and being polar in nature have created γ crystals and mistakenly labelled as β in the literature.

3.3 XRD structural analysis

The structural analysis used the XRD Bruker 8D advanced diffractometer USA. Figure 5 shows the typical XRD profile of the PVDF and its associated composite samples. In our case the pristine PVDF (**P0**) exclusively shows four diffraction peaks at 10.26°, 18.82°, 20.6°, 40.5° and 44.6°, which are customarily assigned to the (100), (020), (110), and (021) reflections of the α-crystal planes [25].

At the same time these cited reflection planes were also assigned to γ form, which makes it difficult to conclude on the phase transformation. The sample designated as **P1** shows reflections at the 10.24°, 20.62°, 40.20° and 44.72° with

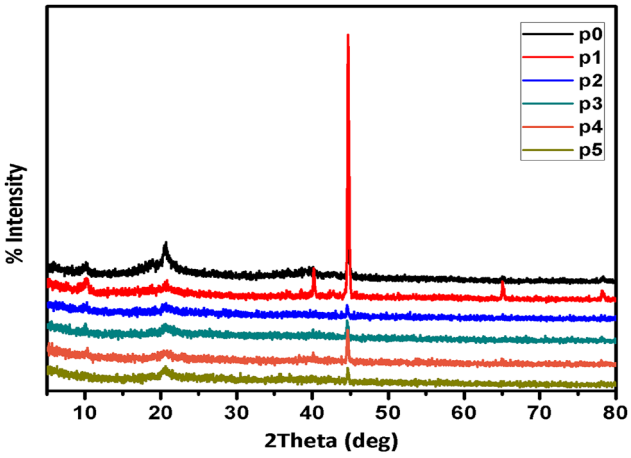

Figure 5: XRD pattern of sample P0, P1, P2, P3, P4, P5.

very small signal near 17.9°, which are exclusively assigned to the β phase in the literature. The emergence of new peaks both in P0 and P1 in the 2θ region of 40–45° may be assigned to the γ or α phase. The signals due to the only IL in PVDF (sample **P2**) show weak intensity at 10.08°, 20.5°, 40.35° and 44.6°. The sample signals from **P3** are centered at 10.08°, 20.5°, 40.07° and 44.6°. The sample **P4** shows reflections at 10.03°, 20.5°, 18.8°, 40.03°, 44.64°. **P5** at 10.08°, 18.8°, 20.5°, 40.4°, and 44.68°.

In the diffraction peaks shown in Figure 5 the signal appears in case P0 is either reduced in size or completely absent in other samples including P1, P2, P3, P4 and P5. This supports the observation that α non- polar fraction has been converted into a polar one. Thus, the IL being polar but incompatible still performs its function of crystal transformation. Some peaks shifting towards higher value also occur and clearly confirm the crystal attenuation. It can also be judged from Figure 5, that in sample P3 to P5 the narrowness of the peak slightly changed to broadness. This may be an indicative of the fact that the amorphous nature of IL loosens the lattice rigidity. Furthermore, micro stresses are produced due to re-alignment of the crystalline phases with increase in the d-spacing gallery and tend to expand the signal.

3.4 Differential scanning calorimetry

DSC was used to determine and record the crystallization and melting history of all samples. The DSC-60 Plus Series Shimadzu Japan was utilized. All samples were heated to 210 °C at the rate of 10 °C/min and kept at the final temperature for 10 min. The samples were then cooled to 25 °C at the same rate and again heated up to 210 °C.

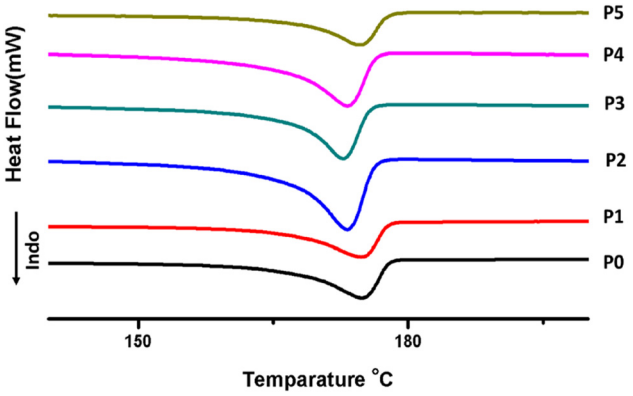

Figure 6: Heating curve for, P0, P1, P2, P3, P4, P5.

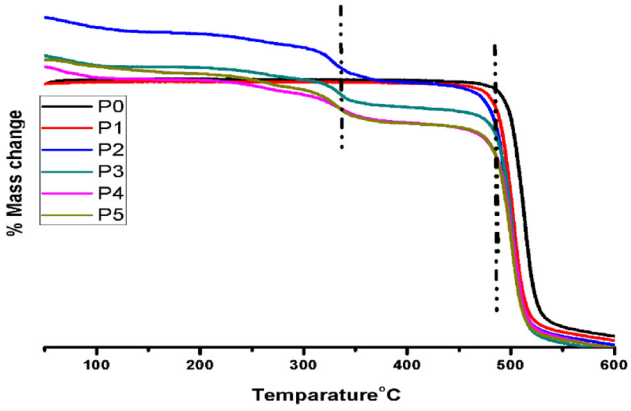

Figure 8: Thermogravimetric curve of sample P0, P1, P2, P3, P4, P5.

Both heating and cooling behavior were recorded. The sample mass was 5.0 mg ± 0.5 in all experiments with continuous nitrogen supply. Here, the addition of MWNT-IL results in the higher melting temperature of P3 samples. It is evident from XRD and FT-IR analysis that the PVDF crystallization extent was increased as well as induction of full polar (β and γ) crystals from the melt state can be achieved via addition of modified MWCNTs to IL in PVDF matrix.

In Figure 6 it is clearly seen that approximately at T_m = 174.3 °C, the melting of pure PVDF is completed. The melting point (T_m) of the P1 sample (175.0 °C) was found to be slightly higher i.e., 1.5 °C than the T_m of neat PVDF (P0).

Upon injection of the IL into the system the T_m significantly depressed and appeared at 173.1 °C, highlighting its plasticizing role. The samples P3, P4 and P5 reveal melting points at 172.84 °C, 173.3 °C, 174.6 °C. In the samples P4 and P5 the role of IL is diminished as indicated by the downward trend. The cooling history of the polymer melt is as drawn in Figure 7. The temperature at which neat PVDF (P0) sample crystallized was recorded at 139.6 °C. The crystallization temperature (T_c) of sample P1, P2, P3, P4 and P5 were recorded at 141.1, 137.8, 138.1, 138.6 and 137.6 °C, respectively. The data reflects the nucleating role of MWCNTs (P1), the plasticizing role of IL (P2) with depression of T_c. Interestingly, when the IL and CNTs are combined they synergistically support each other and push T_c a little further but not too far.

In the case of P5, although the IL concentration was appreciably high, its immiscibility and incompatibility tend to stress the system with dropping of the T_c to the point where only IL was employed.

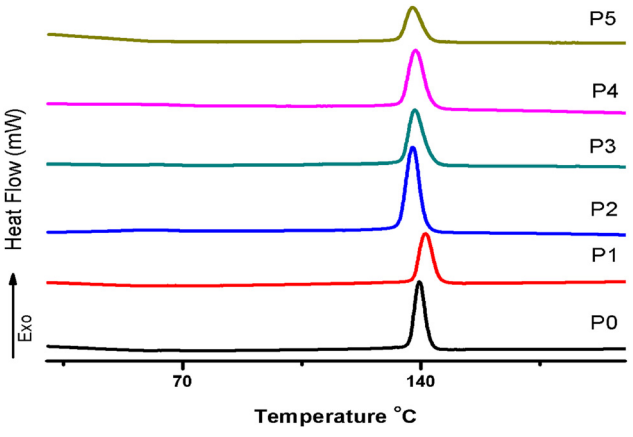

Figure 7: Cooling curve for sample, P0, P1, P2, P3, P4, P5.

3.5 Thermo-gravimetric analysis (TGA)

Thermogravimetric spectra were recorded for P0, P1, P2, P3, P4 and P5 as shown in Figure 8. According to Figure 8 the sample P0 decomposes at ~479 °C, thus highlighting the strength of the polymer. The sample P1 with MWCNTs reinforcement composite decomposed at 472 °C.

Both these decompositions are a single step process. Although, PVDF-MWCNTs-IL (P3, P4, P5) composite exhibits a multistep decomposition mechanism as depicted in Figure 8. First decomposition occurred at ~341 °C while second was observed at ~369 °C. However, it is worth noting that at lower ionic liquid content (up to 20 %), the decomposition temperatures of the polymer and the ionic liquid cannot be distinguished separately [38, 39].

4 Conclusions

The study concludes that the incorporation of multi-walled carbon nanotubes (MWCNTs) into PVDF enhances its overall crystallization behavior by acting as effective nucleating agents. However, MWCNTs alone are insufficient to

significantly promote the formation of desirable electroactive β and γ phases. In contrast, the addition of ionic liquids (ILs), particularly 1-methylimidazolium bromide, and IL-modified MWCNTs has a pronounced effect on PVDF's crystalline phase transformation. The ionic liquid not only improves the dispersion of the filler but also enhances the interaction at the polymer–filler interface, resulting in a synergistic effect that favors polar phase crystallization. The IL presence is critical in facilitating nucleation of electroactive phases by improving compatibility and inducing stronger interfacial interactions.

This study lays the foundation for the design of advanced PVDF-based composite materials with tailored crystalline phases for specific functional applications such as sensors, actuators, and energy harvesting devices. The work emphasizes the role of surface-modified nanofillers and their interfacial interactions with PVDF in directing crystalline phase formation. Future investigations may expand upon this by exploring a broader range of ionic liquids and functionalized nanofillers to further enhance phase selectivity, mechanical properties, and electroactive responses. Additionally, this approach opens new possibilities in the development of high-performance piezoelectric and ferroelectric polymer nanocomposites through synergistic engineering of the filler–matrix interface.

Funding information: This study is supported by Higher Education Commission of Pakistan, the authors extend their appreciation to the Deanship of Research and Graduate Studies at King Khalid University for funding this work through Large Groups Project under Grant No. RGP2/66/46. This work was supported by the Deanship of Scientific Research at Imam Mohammad ibn Saud Islamic University (IMSIU) Saudi Arabia.
Author contributions: Conceptualization, methodology, writing original draft preparation: Fazal Suhrab Gul; Software, validation: Muhammad Azeem, Attiq Ur Rehman; Formal analysis, investigation, resources, data curation, writing review and editing: Antonio Miotello, Khalid Ali Khan, Sara A. Alqarni, Magdi E.A. Zaki; Visualization: Akhtar Munir; Supervision: Zia Ur Rehman; Project administration: Mohsan Nawaz. All authors have accepted responsibility for the entire content of this manuscript and approved its submission.
Conflict of interest: The authors state no conflict of interest.
Data availability statement: All data generated or analysed during this study are included in this published article.

References

1. Inderherbergh J. Polyvinylidene fluoride (PVDF) appearance, general properties and processing. Ferroelectrics 1991;115:295–302.
2. Bahader A, Haoguan G, Nawaz M, Bangesh M, Bangesh F, Ibrar M, et al. Impact of ionic liquid's self-assembly on the crystallization behavior of poly (vinylidene fluoride). J Mol Liq 2019;276:115–9.
3. Zhao X, Li C. Effects of multiwalled carbon nanotubes on phase transformation and dielectric properties in poly (vinylidene fluoride-hexafluoropropylene) nanocomposites. Mater Trans 2019;60: 1716–21.
4. Okada D, Kaneko H, Kato K, Furumi S, Takeguchi M, Yamamoto YJM. Colloidal crystallization and ionic liquid induced partial β-phase transformation of poly (vinylidene fluoride) nanoparticles. Macromolecules 2015;48:2570–5.
5. Linares A, Acosta JJ. Pyro-piezoelectrics polymers materials – I. Effect of addition of PVA and/or PMMA on overall crystallization kinetics of PVDF from isothermal and non-isothermal data. Eur Polym J 1995; 31:615–9.
6. Sencadas V, Gregorio Filho R, Lanceros-Mendez S. Processing and characterization of a novel nonporous poly (vinilidene fluoride) films in the β phase. J Non-Cryst Solids 2006;352:2226–9.
7. Neidhöfer M, Beaume F, Ibos L, Bernes A, Lacabanne CJP. Structural evolution of PVDF during storage or annealing. Polymer 2004;45: 1679–88.
8. Li Y, Liao C, Tjong SC. Electrospun polyvinylidene fluoride-based fibrous scaffolds with piezoelectric characteristics for bone and neural tissue engineering. Nanomaterials 2019;9:952.
9. Salimi A, Yousefi AA. FTIR studies of b-phase crystal formation in stretched PVDF films. Polym Test 2003;22:699–704.
10. Imamura R, Silva A, Gregorio R Jr. γ→ β Phase transformation induced in poly (vinylidene fluoride) by stretching. J Appl Polym Sci 2008;110: 3242–6.
11. Abdullah IY, Yahaya M, Jumali MHH, Shanshool HM. Letters, influence of the substrate on the crystalline phase and morphology of poly (vinylidene fluoride) (PVDF) thin film. Surf Rev Lett 2016;23: 1650005.
12. Sencadas V, Martins P, Pitães A, Benelmekki M, Gomez Ribelles JL, Lanceros-Mendez S. Influence of ferrite nanoparticle type and content on the crystallization kinetics and electroactive phase nucleation of poly (vinylidene fluoride). Langmuir 2011;27:7241–9.
13. Xie L, Huang X, Huang Y, Yang K, Jiang P. Core@ double-shell structured BaTiO3–polymer nanocomposites with high dielectric constant and low dielectric loss for energy storage application. J Phys Chem C 2013; 117:22525–37.
14. Mandal D, Kim KJ, Lee JS. Simple synthesis of palladium nanoparticles, β-phase formation, and the control of chain and dipole orientations in palladium-doped poly (vinylidene fluoride) thin films. Langmuir 2012; 28:10310–7.
15. Huang X, Jiang P, Kim C, Liu F, Yin YJ. Influence of aspect ratio of carbon nanotubes on crystalline phases and dielectric properties of poly (vinylidene fluoride). Eur Polym J 2009;45:377–86.
16. Levi N, Czerw R, Xing S, Iyer P, Carroll DL. Properties of polyvinylidene difluoride – carbon nanotube blends. Nano Lett 2004;4:1267–71.
17. Lee JS, Kim GH, Kim WN, Oh KH, Kim HT, Hwang SS, et al. Crystal structure and ferroelectric properties of poly (vinylidene fluoride)-carbon nano tube nanocomposite film. Mol Cryst Liq Cryst 2008;491: 247–54.
18. Rahman MA, Chung GS. Compounds, synthesis of PVDF-graphene nanocomposites and their properties. J Alloys Compd 2013;581:724–30.
19. Xing C, Zhao M, Zhao L, You J, Cao X, Li Y. Ionic liquid modified poly (vinylidene fluoride): crystalline structures, miscibility, and physical properties. Polym Chem 2013;4:5726–34.

20. Kumar N, Nath R. Current-voltage (IV) characteristics of poly (vinylidene fluoride)/potassium nitrate composite thick film. Integrated Ferroelectrics Int J 2014;158:22–5.
21. Sharma M, Madras G, Bose S. Size dependent structural relaxations and dielectric properties induced by surface functionalized MWNTs in poly (vinylidene fluoride)/poly (methyl methacrylate) blends. Phys Chem Chem Phys 2014;16:2693–704.
22. Mandal A, Nandi AK. Interfaces, ionic liquid integrated multiwalled carbon nanotube in a poly (vinylidene fluoride) matrix: formation of a piezoelectric β-polymorph with significant reinforcement and conductivity improvement. ACS Appl Mater Interfaces 2013;5:747–60.
23. Martins P, Costa CM, Benelmekki M, Botelho G, Lanceros-Mendez S. On the origin of the electroactive poly (vinylidene fluoride) β-phase nucleation by ferrite nanoparticles via surface electrostatic interactions. CrystEngComm 2012;14:2807–11.
24. Chen GX, Zhang S, Zhou Z, Li Q. Dielectric properties of poly (vinylidene fluoride) composites based on bucky gels of carbon nanotubes with ionic liquids. Polym Compos 2015;36:94–101.
25. Xing C, Zhao L, You J, Dong W, Cao X, Li YJT. Impact of ionic liquid-modified multiwalled carbon nanotubes on the crystallization behavior of poly (vinylidene fluoride). J Phys Chem B 2012;116:8312–20.
26. Kabo GJ, Blokhin AV, Paulechka YU, Kabo AG, Shymanovich MP, Magee JW, et al. Thermodynamic properties of 1-butyl-3-methylimidazolium hexafluorophosphate in the condensed state. J Chem Eng Data 2004;49:453–61.
27. Endo T, Kato T, Tozaki K-I, Nishikawa K. Phase behaviors of room temperature ionic liquid linked with cation conformational changes: 1-butyl-3-methylimidazolium hexafluorophosphate. J Phys Chem B 2010;114:407–11.
28. Liang C-L, Mai Z-H, Xie Q, Bao R-Y, Yang W, Xie B-H, et al. Induced formation of dominating polar phases of poly (vinylidene fluoride): positive ion–CF2 dipole or negative ion–CH2 dipole interaction. J Phys Chem B 2014;118:9104–11.
29. Martins P, Lopes A, Lanceros-Mendez S. Electroactive phases of poly (vinylidene fluoride): determination, processing and applications. Prog Polym Sci 2014;39:683–706.
30. Gupta N, Singh Brar B, Woldesenbet E. Effect of filler addition on the compressive and impact properties of glass fibre reinforced epoxy. Bull Mater Sci 2001;24:219–23.
31. Lieberman IH, Togawa D, Kayanja MM. Vertebroplasty and kyphoplasty: filler materials Spine J 2005;5:S305–16.
32. Dizon JRC, Espera AH Jr, Chen Q, Advincula RC. Mechanical characterization of 3D-printed polymers. Addit Manuf 2018;20:44–67.
33. Peng HK, Wang X, Li TT, Lou CW, Wang Y, Lin JH. Mechanical properties, thermal stability, sound absorption, and flame retardancy of rigid PU foam composites containing a fire-retarding agent: effect of magnesium hydroxide and aluminum hydroxide. Polym Adv Technol 2019;30:2045–55.
34. Rao CJ, Venkatesan K, Nagarajan K, Srinivasan T, Rao PV. Electrochemical behavior of europium (III) in N-butyl-N-methylpyrrolidinium bis (trifluoromethylsulfonyl) imide. Electrochim Acta 2009;54:4718–25.
35. Bahader A, Chan S, Nawaz M, Gul FSJD, Treatment W. Preparation and characterization of blended membrane for copper removal application. Desalination Water Treat 2021;231:196–204.
36. Correia De, Barbosa J, Costa C, Reis P, Esperança J, de Zea Bermudez V, et al. Ionic liquid cation size-dependent electromechanical response of ionic liquid/poly (vinylidene fluoride)-based soft actuators. J Phys Chem C 2019;123:12744–52.
37. Barbosa J, Correia D, Gonçalves R, de Zea Bermudez V, Silva M, Lanceros-Mendez S, et al. Enhanced ionic conductivity in poly (vinylidene fluoride) electrospun separator membranes blended with different ionic liquids for lithium ion batteries. J Colloid Interface Sci 2021;582:376–86.
38. Prasad B, Gill FS, Panwar V, Anoop G. Development of strain sensor using conductive poly (vinylidene fluoride)(PVDF) nanocomposite membrane reinforced with ionic liquid (IL) & carbon nanofiber (CNF). Compos B Eng 2019;173:106990.
39. Cao M, Du C, Guo H, Song S, Li X, Li B. Technology, continuous network of CNTs in poly (vinylidene fluoride) composites with high thermal and mechanical performance for heat exchangers. Compos Sci Technol 2019;173:33–40.